



**RESEARCH JOURNAL OF THE DEPARTMENT OF GEOLOGY,
FEDERAL UNIVERSITY OF TECHNOLOGY, MINNA, NIGERIA**



MINNA JOURNAL OF GEOSCIENCES

The Maiden Edition: Volume 1 Number 1

TABLE OF CONTENTS

Finite Element Discretization and Simulation of Groundwater Flow System	1 – 10
Shehu, M. D., Adeboye, K. R. and Ndanusa, A.	
Deep Water Planktic Foraminifera Biostratigraphy of the Western Niger Delta, Nigeria	11 – 24
Okosun, E. A. and Chukwuma-Orji, J. N.	
Geospatial Analysis of Urbanization Trend and its Effects on the Vegetal Cover of Jos South Local Government Area of Plateau State, Nigeria	25 – 40
Muhammed, M., Joseph, M. M. and Hassan, A.B.	
Major Oxides Geochemistry of some Tourmalines from Southwestern Nigeria	41 – 64
Olatunji, A. S. and Jimoh, R. O.	
Evaluation of Depth to Magnetic Basement over Sokoto Basin, Northwestern Nigeria Using Spectral Fourier Analysis of High Resolution Aeromagnetic Data	65 – 76
Shehu, A. T., Nwankwo, L. I. and Salako, K. A.	
Investigating the Quality of Groundwater from Hand-dug Wells in Lapai, Niger State using Physico-chemical and Bacteriological Parameters	77 – 92
Amadi, A.N., Olasehinde, P.I., Obaje, N.G., Unuevho, C.I., Yunusa, M.B., Keke, U.N. and Ameh, I.M.	
Impact of Geology on the Stability of Minna-Lambata Road, North Central Nigeria	93 – 106
Waziri, S.H., Wazirim, N.M., Ako, T.A., Alabi, A.A. and Abdulfatai, I.A.	
Compositional Characteristics and Petrogenetic Features of Metasedimentary Rocks of Zungeru Area Northwestern Nigeria	107 – 120
Alabi, A. A., Garba, I., Danbatta, U.A., Najime, T.	
Anastomosing River Deposits: A Case Study of Enagi Siltstone, Northern Bida Basin, Central Nigeria	121 – 134
Goro, A. I., Okosun, E. A., Akande, W. G. and Salihu, H. D.	
Palynological Studies of Wells A-1 and B-1, Western Niger Delta, Nigeria	135 – 148
Aluko, C., Okosun, E. A. and Onoduku, U. S.	
Geoelectrical Prospecting for Regolith Aquifer in Kundu, Zungeru Sheet 163, Nigeria	149 – 164
Tswako, M., Unuevho, C.I., Okeugo, C. G., Amadi, A.N., Ejepu, J. S. and Onuoha, K.M.	

Palynological Evidence of a Campanian-Maastrichtian Boundary in
Nigeria: Implication for Paleoenvironment, Paleoclimate and Hydrocarbon
Prospectivity
Onoduku, U.S., Okosun, E.A., *Obaje, N. G., Goro, A.I., Salihu, H.D. and
Chukwuma-Orji, J. N. 165 – 178

An Evaluation of Chemical Quality of Groundwater in a Contact Geological Terrain: A
Case Study of Lapai, North Central Nigeria
Ojieriakhi, S. A., Idris-Nda, A. and Waziri, N.M. 179 – 196

Geotechnical Assessment of Causes of Structural Failure in Parts of Minna, Central
Nigeria
Umar, M. U., Idris-Nda, A. and Okunlola, I.A. 197 – 210

Evaluation of Depth to Magnetic Basement over Sokoto Basin, Northwestern Nigeria Using Spectral Fourier Analysis of High Resolution Aeromagnetic Data

¹Shehu, A. T., ²Nwankwo, L. I. and ³Salako, K. A.

¹Physics Unit, Centre for Preliminary and Extra-Mural Studies, Federal University of Technology Minna, Niger State, Nigeria.

²Department of Physics, University of Ilorin, Kwara State, Nigeria.

³Department of Physics, Federal University of Technology Minna, Niger State, Nigeria.

*Correspondence Author: atshehu2006@gmail.com

Abstract

Fourier analysis of High Resolution Aeromagnetic Magnetic (HRAM) data was carried out to evaluate depth to the magnetic basement of the entire Sokoto Basin in northwestern Nigeria to infer hydrocarbon potential for sustainable economy. The area covered is approximately 111,925 km² and is bounded by Latitudes 10.00°N and 14.00°N Longitudes 3.50°E and 7.00°E. It is covered by 38 Sheets of aeromagnetic data joined to produce composite TMI map. The composite data was then divided into thirty seven sections of half degree by half degree for the purpose of two-dimensional spectral analysis in order to estimate sedimentary depth underlain by the magnetic basement rock in the area. Results of the spectral analysis suggested the existence of two clear layers of magnetic sources which account for deeper and shallower magnetic sources. Linear segment from the low frequency portion of the spectral plot is due to deeper source effects. The deeper sources vary between 0.47±0.04 km - 3.08±0.05 km with an average of 1.94±0.07 km and these deeper sources represented by the low frequency component of the spectrum are considered to be the thickness of the sedimentary formation. The sedimentary thickness increases from the south to north. The shallow layer depths vary from 0.12±0.03 km – 1.09±0.07 km with an average of 0.47±0.03 km represent the near surface sources. Lema with sedimentary thickness up to 3.0 km is a probable area for hydrocarbon generation and is recommended for detailed seismic survey and soil sample tests. These results agree with earlier geophysical works done in parts of the area.

Keywords: Basement depth, HRAM (high resolution aeromagnetic data), Magnetic sources Hydrocarbon and Sokoto basin.

Introduction

The Sokoto Basin in Northwestern Nigeria consists predominantly of a gentle undulating plain, unconformably underlain by basement rocks consisting of igneous and metamorphic rocks. This sedimentary basin like other sedimentary basins in Nigeria could serve as primary host for hydrocarbon if properly explore for economic reasons. This work aimed at exploring for hydrocarbon potential in the entire Sokoto basin is in line with government effort to diversify

hydrocarbon exploitation beyond Niger Delta region of Nigeria for sustainable economy capable of solving the current economic recession in Nigeria. It is also capable of reducing the exploration and exploitation risk in the southsouthern part of the country. The high resolution aeromagnetic anomaly data from the nationwide airborne survey of 2009 reflects the lateral variation in the earth's magnetic field. These variations are related to changes of structure, susceptibility of magnetic materials in the crust used in this study is digital and has a higher resolution than that used by earlier study in the area, moreover the study covers the entire basin unlike the previous work in the study area that covers parts of the study area. The High Resolution Airborne Geophysical Digital Data were acquired from Nigerian Geological Survey Agency in airborne survey using aircrafts flown at height of 80 m with 500 m line spacing, 80 m mean terrain clearance and the tie line spacing of 500 m. This new low height survey data has been adjudged to be better than the previous 1970's low resolution analogue data by the NGSA (Nwankwo and Shehu, 2015). Geophysical work using HRAM data on this topic in this area were lacking, hence this work filled the gap of lacking digital baseline data for hydrocarbon exploration for economic reasons in Nigeria.

Location and Geology of the Study Area

The Sokoto Basin located in the northwestern part of Nigeria is bounded by latitudes 10.00° N and 14.00° N and longitudes 3.50° E and 7.00° E (Figure 1). It has a total surface area of approximately $111,925 \text{ km}^2$, which cuts across six states in Nigeria namely: Kaduna, Katsina, Kebbi, Niger, Sokoto and Zamfara, and it is one of the inland basins in Nigeria. It is a sedimentary basin and consists of gentle undulating plain, underlain by basement rocks consisting of igneous and metamorphic rocks.

The Sahel climate or tropical dry climate which is the predominant climate type in the area is dominated by two opposing air masses, tropical maritime and tropical continental. The tropical maritime is wet and blows from the Atlantic ocean while the tropical continental air, which is dry blows from the Sahara desert.

Previous works have shown that Sokoto Basin is a region with great potential for future large-scale economic development, due to warm and bountiful mineral resources, geothermal energy from natural heat sources closed to the land surface. The most important economics mineral in the Sokoto Basin are the industrial minerals consisting of clays, limestone, gypsum and phosphate others include ironstones, laterites, gravel and lignite.

Sokoto Basin in the northwestern Nigeria constitutes the southeastern portion of the lullemeden Basin, which extends from Mali and the western boundary of Niger republic through northern Benin Republic and Northwestern Nigeria into Eastern Niger Republic and it covers an area of about $800,000 \text{ km}^2$.

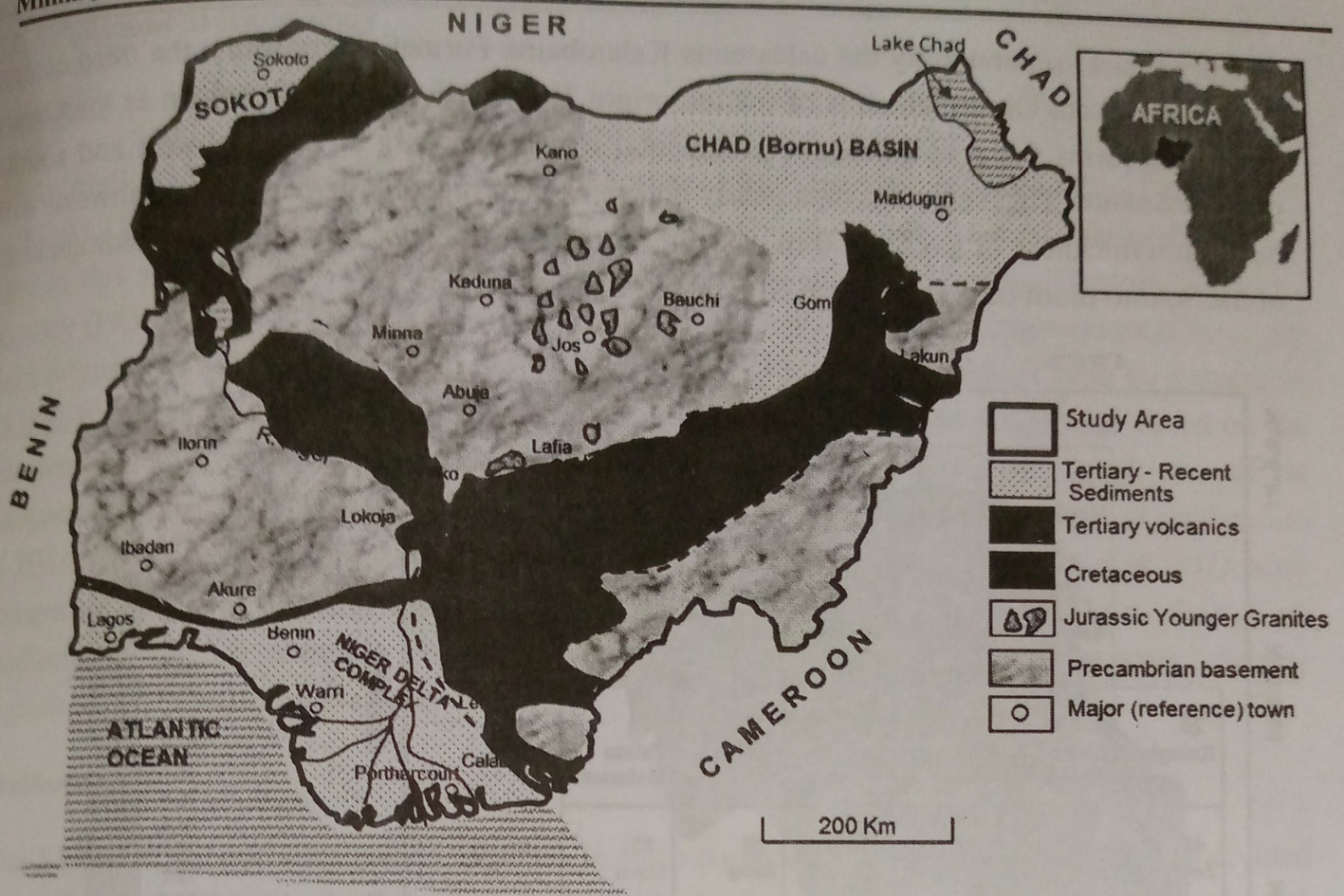


Figure 1: Geological map of Nigeria showing Sokoto Basin (Modified after Obaje *et al.*, 2004).

The rock units are predominantly clay alternating with gritty sand unit, they are ill-sorted, poorly consolidated with gravel overlying the Precambrian basement uncomfortably, consist of a gentle undulating plain with an average elevation varying from 250 to 400m above sea-level this plain is occasionally interrupted by low mesas, a low escarpment, known as the Dange scarp; is the most prominent feature in the basin and it is closely related to the geology, the Nigerian Sector of the lullemeden Basin is underlain by basement rock consisting of igneous and metamorphic rocks. The basement is directly overlain by Cambrian beds to the north in the Tassaili and the Hoggar mountains. As one traverses the basin from the north towards the southwest the formations become younger in age and rest directly on the Precambrian basement. This situation is referred to as an overlap where progressively younger beds rest upon the older series (Kogbe, 1979). The sediments of the Sokoto basin were deposited under varied environmental situations ranging from continental to marine events. The sedimentary rocks in the basin have been classified under four major categories. Overlying the Precambrian basement unconformably is the first category is known as the Illo and Gundumi Formations, made up of grits and clays. They are overlain uncomfortably by the second category known as Maastrichtian Rima Group, consisting of mudstone and friable sandstone (Taloka and Wurno Formations) separated by the fossiliferous, Shelly Dukamaje Formation. The Dange and Gamba Formations

(mainly shales) separated by the calcareous Kalambaina Formation constitute the third category known as Sokoto Group which is of marine origin. The fourth category is known as the Gwandu Formation forms the post-Paleocene continental terminal occurs in the northwest and southern parts of Sokoto. This sediment dips gently and thickens gradually towards the northwest, with a maximum thickness of over 1,200 m near the frontier with Niger Republic. The geological map of the Sokoto basin of northwestern Nigeria is shown on Figure 1.

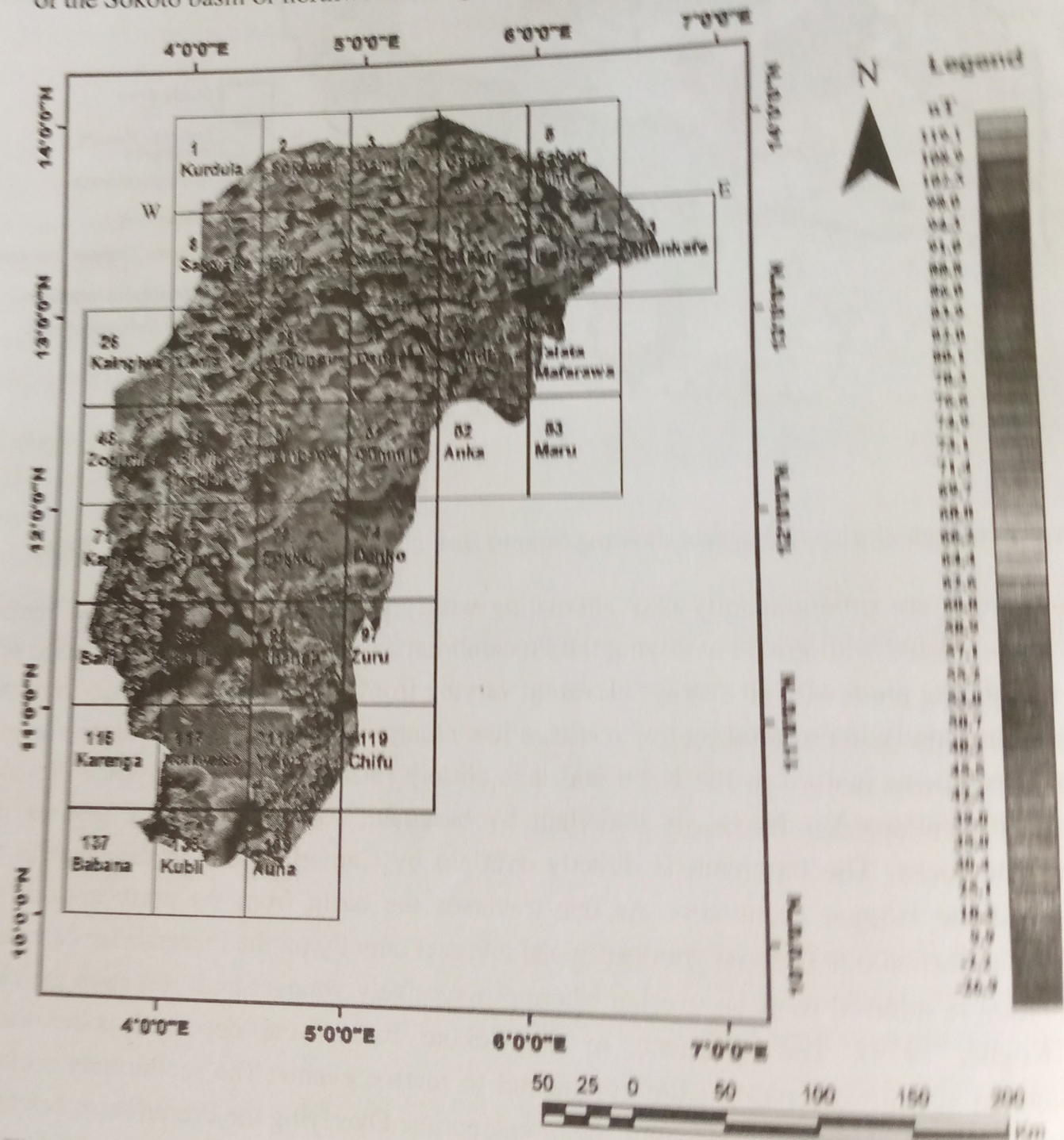


Figure 2: Total magnetic intensity map (TMI) of entire Sokoto basin with superimposed Federal Survey half degree sheets and showing major towns flown over. A constant 33,000 NanoTesla (nT) removed.

Materials

Thirty eight (38) digital half degree HRAM maps (sheet number 1-5, 8-13, 26-31, 48-53, 71-74, 94-97, 116-119 and 138-139) on a scale of 1:100,000 with a total 7,426,917 data points were used in this study. The whole data, which were procured from the Nigerian Geological Survey Agency (NGSA), Oasis Montaj Software was used to assemble data into composite total magnetic field intensity (TMI) map (2), it ranges between 32,487.96 and 33,423.06 nT with an average of 33,060.70 nT and a standard deviation of 38.314. Regional correction which was based on the International Geomagnetic Reference Field (IGRF model 11 of 2015) was made as well as subtraction of a constant TMI value of 33,000 nT by the NGSA before the eventual publication as HRAM Maps. No further processing was made for the reason that Ravat *et al.* (2007), after comparing different spectral methods of estimating depth to the magnetic sources from high resolution magnetic anomaly data, strongly recommended that filtering to remove arbitrary regional fields should be avoided.

Methodology

The Magnetic sheets were joined together to form composite TMI data (2) which was divided into thirty eight (38) blocks for the purpose of 2D spectral analysis while ensuring that essential parts of the anomaly were not cut out by the blocks. Each block covers a square area of 55 km x 55 km. If the source bodies have bases deeper than $L/2\pi$, they may not be appropriately resolved by spectral method (Shuey *et al.*, 1977). Therefore, data window of 50 x 50 km will satisfactorily resolve depth information to a depth of 7.96 km. This window size was selected on the basis of previous studies (Bonde *et al.*, 2014) and Nwankwo and Shehu (2015). However, sheet number 53 (Maru) with insufficient data was omitted. Hence, data in each of the thirty seven (37) blocks was Fast Fourier Transformed (FFT) and radially averaged power spectrum obtained using geosoft Oasis montaj. This produced column for logs of energy and the corresponding frequencies. Energy spectrum plots were plotted for each of the thirty seven blocks, (3) shows azimuthally averaged energy spectra for blocks 14, 19, 30 and 37. Bhattacharyya and Leu (1976) showed that energy spectrum expresses the total magnetic field intensity over a single rectangular block whose depth, width and thickness of the magnetic source ensemble affects the shape of the energy spectrum. Consequently, plots of energy spectrum shows the rate of decay of the spectrum. Linear segment from the low frequency portion of the spectral plot, representing contributions from the deep-seated magnetic sources could be estimated from the slope of each energy spectral plot and subsequently was used to estimate H2 using equation 13, while slope of the linear segment from the high frequency portion of each plots were used to estimate depth H1 (Table 1). The H2 is the thickness of the

sedimentary fill on top of the basement, this estimates could also be used for locating major structures in basement rocks.

Theory of Spectral Analysis

Spectral Fourier analysis was applied out on the high resolution aeromagnetic data. The Fourier Transform is represented mathematically as shown below:

$$f(t) = a_0 + \sum_{n=1}^{\infty} (a_n \cos nt + b_n \sin nt) \quad (1)$$

$$a_0 = \frac{1}{2} \int_{-\pi}^{\pi} f(t) dt \quad (2)$$

$$a_n = \frac{1}{\pi} \int_{-\pi}^{\pi} f(t) \cos nt dt \quad (3)$$

$$b_n = \frac{1}{\pi} \int_{-\pi}^{\pi} f(t) \sin nt dt \quad (4)$$

where a_0 , a_n and b_n are Fourier coefficients and their estimations is referred to as Fourier analysis. $n = 0, 1, 2, 3, \dots$

This geophysical analysis is commonly applied on regularly spaced data such as aeromagnetic data using Discrete Fourier Transforms (Spector and Grant, 1970; Hahn, 1976; Murthy and Mishra, 1980):

$$f(n) = F(n) e^{j\phi(n)} \frac{1}{N} \sum_{u=1}^N f(u) e^{-j(\frac{2m\pi n}{N})u} \quad (5)$$

where the given time series are $f(1), f(2), \dots, f(N)$ for N data points, at equal spacing.

In magnetic analysis, it is useful to have proposed models, such as sphere, cylinders and faults which cause the anomaly at the surface. For this reason, the total magnetic field anomaly ΔT , measured in the direction of geomagnetic field is given by (Spector and Grant, 1970; Hahn, 1976; Murthy and Mishra, 1980):

$$T = \frac{1}{2} A \left[\ln \frac{(x-t \cot d)^2 + (h+t)^2}{x^2 + h^2} + B \left[\tan^{-1} \left\{ \frac{(x-t \cot d)}{(h+t)} \right\} - \tan^{-1} \left(\frac{x}{h} \right) \right] \right] \quad (6)$$

where $A = 2kH_o(1 - \cos^2 i \cos^2 h\lambda) \sin d \cos(d - 2\beta)$ and

$B = 2kH_o(1 - \cos^2 i \cos^2 h\lambda) \sin d \sin(d - 2\beta)$, I = magnetic inclination, d = dip of the step, t = thickness of the step, k = susceptibility constant, H_o = geomagnetic field and the angle I and h are combined into a single variable defined by $\tan \beta = \tan i / \sin \lambda$.

The Fourier transform and modified transform of equation (8) is given respectively as:

$$\Delta T(\omega) = \frac{\pi}{\omega} e^{-h\omega} [(A - A \cos(t\omega \cot d) e^{-t\omega} - B \sin(t\omega \cot d) e^{-t\omega} - j \cos(t\omega \cot d) e^{-t\omega} - A \sin(t\omega \cot d) e^{-t\omega} - B] \quad (7)$$

$$\Delta T(\omega) = \pi e^{-h\omega} [A - A \cos(t\omega \cot d) e^{-t\omega} - B \sin(t\omega \cot d) e^{-t\omega} + j \cos(t\omega \cot d) e^{-t\omega} - A \sin(t\omega \cot d) e^{-t\omega} - B] \quad (8)$$

The modified Amplitude Spectrum is consequently given by

$$A(\omega) = C e^{-h\omega} (1 + e^{-2t\omega} - 2 \cos(t\omega \cot d) e^{-t\omega}) \frac{1}{2} \quad (9)$$

Where $C = 2\pi K H_o (1 - \cos^2 i \cos^2 \lambda) \sin d$

Taking the logarithm of equation (9):

$$\ln A(\omega) = \ln C - m\omega + \frac{1}{2} \ln [1 + e^{-2t\omega} - 2 \cos(t\omega \cot d) e^{-t\omega}] \quad (10)$$

For sufficiently larger value of ω , equation (10) reduces to:

$$\ln A(\omega) = \ln C - m\omega \quad (11)$$

Where $\ln A(\omega)$ is energy spectrum and ω is frequency (cycle/km).

The depth h to the causative bodies can subsequently be calculated using the relation (Spector and Grant, 1970):

$$h = -\frac{m}{4\pi} \quad (12)$$

In this work, the graph of $\ln A(\omega)$ against frequency (ω) was plotted and the gradient (m_1) for the deeper source and gradient (m_2) for shallow source were deduced. The depths h_1 and h_2 are therefore given by the respective slopes of straight line segments of low and high frequency portions of energy spectrum (Spector and Grant, 1970; Hahn, 1976; Murthy and Mishra, 1980):

$$h_1 = \frac{m_1}{4\pi} \text{ and } h_2 = \frac{m_2}{4\pi} \quad (13)$$

Results and Discussion

The exponential rate of decay of magnetic power signal is expressed in the graph of log of spectral energy against frequency; energy spectral plots for the thirty seven blocks were plotted and these forms the bases for evaluation of shallow sources depth (H_1) and deeper sources depth (H_2) using equation 13, plots for some selected blocks are shown in Figure 3.

The result obtained from the plot of log of spectral energies against frequency for various blocks. Table 1 gives estimates of depth to magnetic sources. The table shows that the deeper magnetic sources H_2 vary between 0.47 ± 0.04 km - 3.08 ± 0.95 km with an average of 1.95 ± 0.97 km, while the shallow magnetic sources (H_1) vary between 0.12 ± 0.03 km - 1.09 ± 0.97 km with an average of 0.47 ± 0.03 km. The results agree with previous depth to shallow magnetic sources of 0.22 - 0.96 km with an approximate average value of 0.46 km obtained by (Adetona *et al.*, 2007). The magnetic basement depth, i.e., crustal thicknesses agree with the estimated 1.00 - 3.00 km (Obay *et al.*, 2013) and 1.23 - 3.10 km (Bonde *et al.*, 2014). The result also agree with documented data (Figure 2) from Nigerian Geological Survey Agency Abuja-Nigeria, low magnetic anomalies areas correspond to sections with high sedimentary thickness due to basement top depression while high magnetic anomalies area correspond to sections with low sedimentary thickness as evidenced in blocks 23 and 24. The sedimentary thickness increases from the south to the north as shown in Figure 4. Crustal thickness map generated from the values of H_2 . Areas with sedimentary thickness value of 3.00 km or above indicate potential for oil and gas (Olaye *et al.*, 2014) if other conditions for hydrocarbon generation are favorable. Nwankwo and Sulu (2015) has also shown that the northcentral parts of the study area have great geothermal gradient from shallow resources as shown in Figure 5, this area correspond to area where the sedimentary fill is up to 3.0 km.

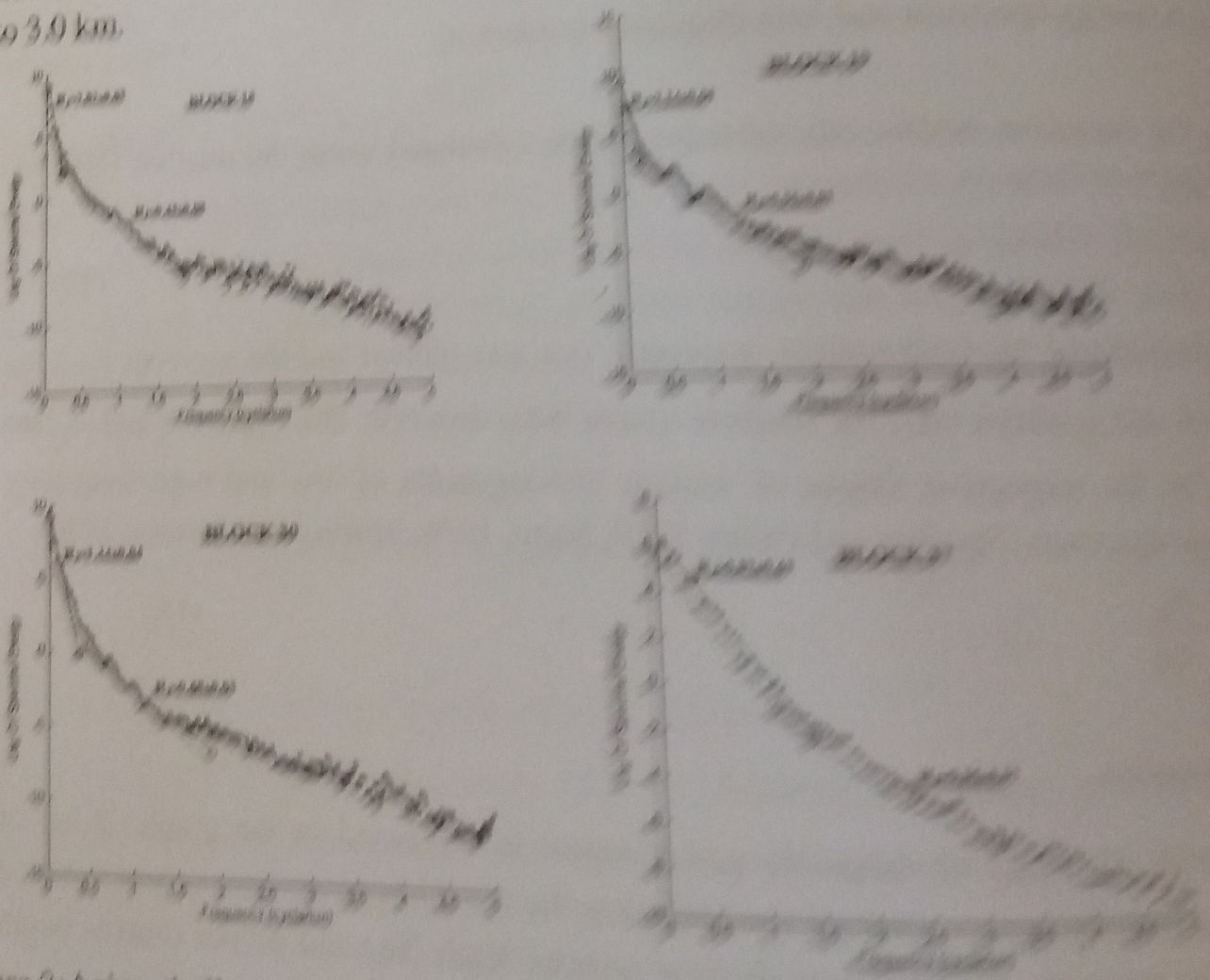


Figure 3: Azimuthally averaged energy spectra for blocks, 16, 19, 30 and 31.

Block 13 (Lema) with highest sedimentary fill on the basement is the most probable area in the basin for hydrocarbon (oil and gas) exploration.

Statistically, the sedimentary fill on the basement in the other area within the northern parts of the study area are thick but not up to 3.0 km correspond to areas with high geothermal gradient is immature for oil but mature for gas. The northern part of the study area would be highly prospective for gas due to high geothermal gradient in the area. Figure 4 is the contour map of estimated second magnetic layer (H_2) depth contour interval of 0.10 km of the study area, portion filled in yellow represent areas with fairly high sedimentary thickness found in the northern part of the study area while area filled in black color represent areas with low sedimentary thickness found in the southern part of the study area. Figure 6 is the Basement topographic map of the second layer (H_2) depth shows that the sedimentary fill on top of the basement in the northern part is thicker than the southern part, interpreted to corresponds to many troughs, trenches, ditches, sinks, pits and holes (indicated in brown), while the southern part (indicated in blue) corresponds to basement high (ridge) with low sedimentary fill on the basement. The maps (Figures 4 and 6) are trending NE-SW in the northern part and NW-SE trending in the southern part. The observed trends are similar to the regional trending faults in the basin which are prominent at Dange and Gilbedi, where the palaeocene beds have been truncated by several WSW-ENE faults (Kogbe, 1979 and Wright *et al.*, 1985).

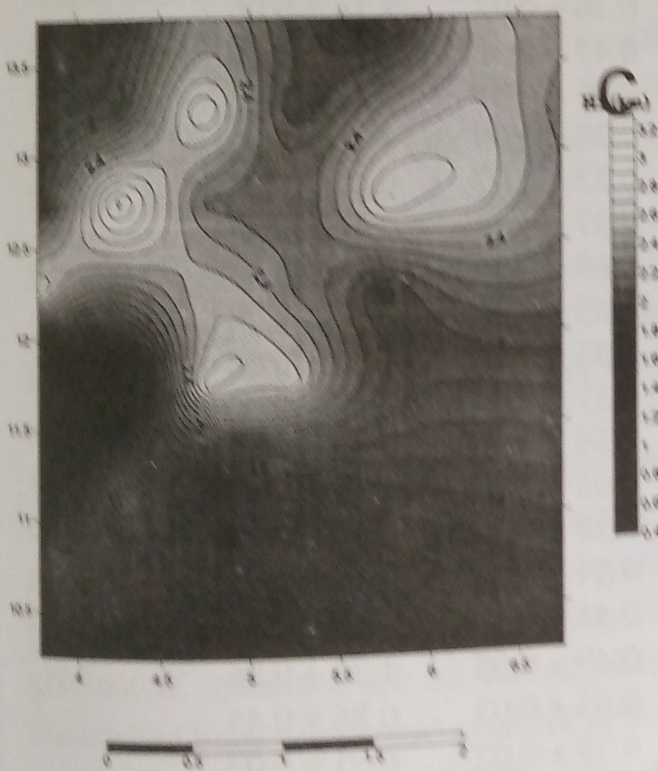


Figure 4: Contour Map of estimated second magnetic layer (H_2) depth Contour Interval of 0.10 km of the study area.

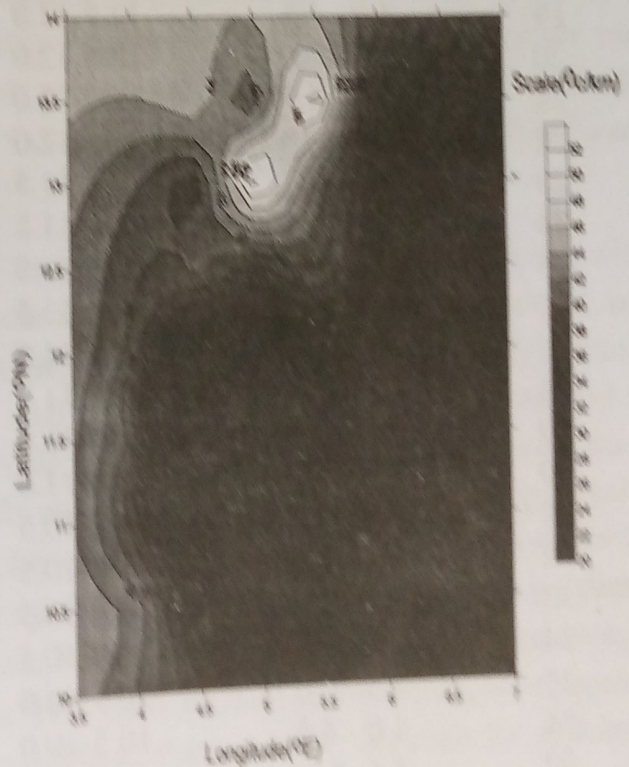


Figure 5: Geothermal gradient map of the study area (contour interval 2.0 °C/km) (Nwankwo and Shehu, 2015).

Table 1: Estimates of depths to magnetic sources.

Blocks	Longitude($^{\circ}$ E)	Latitude($^{\circ}$ N)	H ₁ (Km)	H ₂ (Km)
1	4.0 - 4.5	14.0-13.5	0.48 \pm 0.03	1.84 \pm 0.04
2	4.5- 5.0	14.0-13.5	0.48 \pm 0.23	2.32 \pm 0.06
3	5.0 - 5.5	14.0-13.5	0.38 \pm 0.02	2.08 \pm 0.08
4	5.5- 6.0	14.0-13.5	0.32 \pm 0.01	1.76 \pm 0.23
5	6.0 - 6.5	14.0-13.5	0.28 \pm 0.13	2.54 \pm 0.45
6	4.0 - 4.5	13.5-13.0	0.27 \pm 0.02	1.94 \pm 0.34
7	4.5- 5.0	13.5-13.0	0.55 \pm 0.06	2.82 \pm 0.12
8	5.0 - 5.5	13.5-13.0	0.12 \pm 0.03	2.02 \pm 0.14
9	5.5- 6.0	13.5-13.0	0.72 \pm 0.02	2.43 \pm 0.33
10	6.0 - 6.5	13.5-13.0	0.84 \pm 0.05	2.62 \pm 0.15
11	6.5 - 7.0	13.5-13.0	0.31 \pm 0.02	2.34 \pm 0.08
12	3.5 - 4.0	13.0-12.5	0.32 \pm 0.02	1.93 \pm 0.04
13	4.0 - 4.5	13.0-12.5	1.09 \pm 0.07	3.08 \pm 0.05
14	4.5- 5.0	13.0-12.5	0.76 \pm 0.02	2.28 \pm 0.08
15	5.0 - 5.5	13.0-12.5	0.30 \pm 0.03	2.20 \pm 0.09
16	5.5- 6.0	13.0-12.5	0.43 \pm 0.08	2.82 \pm 0.63
17	6.0 - 6.5	13.0-12.5	0.47 \pm 0.23	2.67 \pm 0.27
18	3.5 - 4.0	12.5-12.0	0.41 \pm 0.05	2.74 \pm 0.41
19	4.0 - 4.5	12.5-12.0	0.36 \pm 0.02	2.14 \pm 0.06
20	4.5- 5.0	12.5-12.0	0.45 \pm 0.06	2.58 \pm 0.03
21	5.0 - 5.5	12.5-12.0	0.35 \pm 0.01	2.28 \pm 0.02
22	5.5- 6.0	12.5-12.0	0.35 \pm 0.05	1.85 \pm 0.02
23	3.5 - 4.0	12.0-11.5	0.22 \pm 0.07	0.47 \pm 0.04
24	4.0 - 4.5	12.0-11.5	0.37 \pm 0.14	0.59 \pm 0.08
25	4.5- 5.0	12.0-11.5	0.89 \pm 0.23	2.75 \pm 0.05
26	5.0 - 5.5	12.0-11.5	0.55 \pm 0.05	2.65 \pm 0.04
27	3.5 - 4.0	11.5-11.0	0.33 \pm 0.01	0.74 \pm 0.08
28	4.0 - 4.5	11.5-11.0	0.57 \pm 0.03	1.68 \pm 0.52
29	4.5- 5.0	11.5-11.0	0.56 \pm 0.06	1.34 \pm 0.35
30	5.0 - 5.5	11.5-11.0	0.68 \pm 0.03	1.44 \pm 0.04
31	3.5 - 4.0	11.0-10.5	0.28 \pm 0.02	1.80 \pm 0.08
32	4.0 - 4.5	11.0-10.5	0.34 \pm 0.01	1.50 \pm 0.06
33	4.5- 5.0	11.0-10.5	0.41 \pm 0.04	1.46 \pm 0.09
34	5.0 - 5.5	11.0-10.5	0.49 \pm 0.05	1.32 \pm 0.06
35	3.5 - 4.0	10.5-10.0	0.63 \pm 0.03	0.86 \pm 0.45
36	4.0 - 4.5	10.5-10.0	0.39 \pm 0.02	0.91 \pm 0.03
37	4.5- 5.0	10.5-10.0	0.36 \pm 0.02	0.82 \pm 0.63
Average			0.47 \pm 0.03	1.93 \pm 0.07

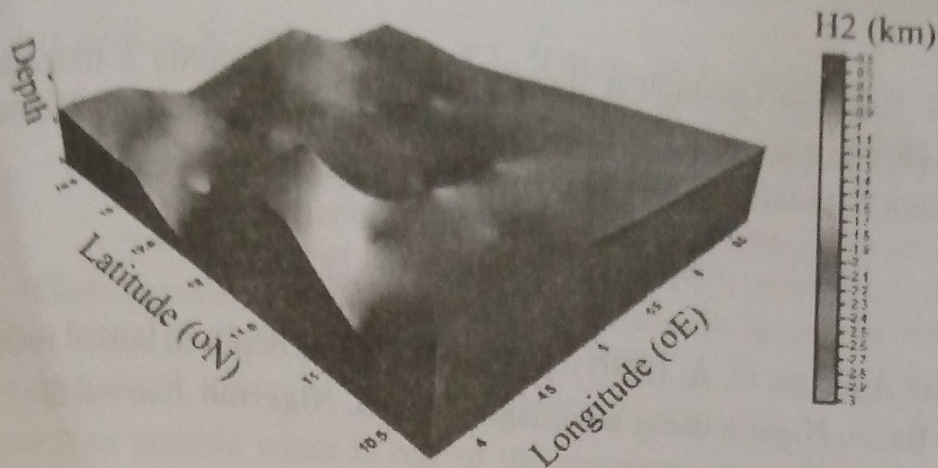


Figure 6: Basement topographic map of the second layer layer (H2) depth.

Conclusions

The result of the spectral analysis of the high resolution regional aeromagnetic data over the entire Sokoto Basin suggested the existence of two clear layers of magnetic source. The deeper sources vary between 0.47 ± 0.04 km - 3.08 ± 0.05 km with an average of 1.94 ± 0.07 km, these deeper sources effect represented by the low frequency component of the energy spectrum are considered to be the thickness of the sedimentary formation. The shallow layer depth varies between 0.12 ± 0.03 km - 1.09 ± 0.07 km with an average of 0.47 ± 0.03 km and these shallow sources effect represented by the high frequency component of the energy spectrum represents the near surface contribution.

It has been shown in previous works that minimum sedimentary thickness of 3.00 km with a threshold depth temperature of 115°C is required for oil accumulation provided all other hydrocarbon generation conditions are favorable for oil formation. Base on this likely condition, probable area for fossil fuel energy (oil and/or gas) is block 13 (Lemu) which correspond to a sink as can be inferred in basement topographic map (Figure 6). However, it is commonly known that high geothermal gradient enhances early formation of gas or oil. Consequently it can be concluded that Lemu is the only probable area for oil and gas exploration while most northern parts of the study area with sedimentary fill not up to 3.0 km but correspond to high geothermal gradient is immature for oil due to shallow crustal thickness, but mature for gas owing to established high geothermal gradient in the area. This work on evaluation of magnetic basement depth revealed that energy options exist in Sokoto Basin that could be explored for sustainable economy. The observed probable area, Lema, is recommended for detailed hydrocarbon exploration using seismic geophysical method.

Acknowledgments

The authors are grateful to the Nigerian Geological Survey Agency for granting a financial rebate on the purchase of the HRAM data, and the Federal University of Technology, Minna-Nigeria for granting the lead author a research leave to undertake the study.

References

- Adetona, A. A., Udensi E. E. and Agelaga, G. A. (2007). Determination of depth to buried rocks under the lower Sokoto Basin, Nigeria using aeromagnetic data. *Nigerian Journal of Physics*, 19: 275-283.
- Bhattacharyya, and Leu (1976). Spectral analysis of gravity and magnetic anomalies due to two dimensional structures. *Geophysics*, 40: 993-1031.
- Bonde, D.S., Udensi, E.E., Momoh, M., Joshua, B.W and Abbas, M. (2014). Basement Depth Estimates of Sokoto Sedimentary Basin, Northwestern Nigeria, Using Spectral Depth Analysis. *SGJ of Geology and Exploration Research*, 1 (4): 78-85.
- Hahn, A. E., kind, G. and Mishra, D.C. (1976). Depth estimation of magnetic source by means of Fourier Amplitude Spectra. *Geophysical Prospecting*, 24: 287.
- Kogbe, C. A. (1979). Geology of the Southeastern (Sokoto) sector of the Iullemeden Basin. *Bulletin, Department of Geology, Ahmadu Bello University*, 2(1): pp. 91 -237.
- Murthy, K. S. R. and Mishra, D. C. (1980). Fourier transform of the general expression for the magnetic anomaly due to a long horizontal cylinder. *Geophysics*, 45, 1091 -1093.
- Nwankwo, L. I. and Shehu, A. T. (2015). Evaluation of Curie-point depths, geothermal gradients and near-surface heat flow from high-resolution aeromagnetic (HRAM) data of the entire Sokoto Basin, Nigeria. *Journal of Volcanology and Geothermal Research*, 305, 45-55. Publisher, Elsevier.
- Obaje, N. G., Aduku, M. and Yusuf I. (2014). The Sokoto Basin of Northwestern Nigeria: A Preliminary Assessment of the Hydrocarbon prospectivity. *Petroleum Technology Development Journal*, 3 (2): 66 – 80.
- Ravat, D., Pignatelli, A., Nicolosi, I. and Chiappini, M. (2007). A study of spectral methods of estimating the depth to the bottom of magnetic sources from near-surface magnetic anomaly data. *Geophysical Journal International*, 169(2): 421 – 434.
- Shuey, R.T., Schellinger, D.K., Tripp, A.C., Alley, L.B. (1977). Curie depth determination from aeromagnetic spectra. *Geophys. J. R. Astron. Soc.*, 50: 75-101.
- Spector, A. and Grant, F. S. (1970). Statistical models for interpreting aeromagnetic data. *Geophysics*, 35: 293 – 302.
- Wright, J. B., Hastings, D., Jones, W. B. and Williams, H. R. (1985). *Geology and Mineral Resources of West Africa*. George Allen and Urwin, London, 90 – 120.